

Effect of phase mask alignment on fiber Bragg grating spectra at harmonics of the Bragg wavelength

Scott A. Wade,¹ William G. A. Brown,¹ Harpreet K. Bal,² Fotios Sidirolou,²
Greg W. Baxter,² and Stephen F. Collins^{2,*}

¹CAOUS, Swinburne University of Technology, Hawthorn, VIC 3122, Australia

²Optical Technology Research Laboratory, School of Engineering and Science, Victoria University,
PO Box 14428, Melbourne, VIC 8001, Australia

*Corresponding author: stephen.collins@vu.edu.au

Received December 21, 2011; revised June 25, 2012; accepted June 27, 2012;
posted June 27, 2012 (Doc. ID 160392); published July 19, 2012

Effects of fabrication conditions on the double-peak structure observed in fiber Bragg gratings at harmonics of the Bragg wavelength were investigated, showing that slight variations in the alignment of the phase mask can affect the grating spectra significantly. A single peak occurs only when the incident beam direction is perfectly normal with respect to the fiber. © 2012 Optical Society of America

OCIS codes: 060.3735, 070.6760, 050.2770.

1. INTRODUCTION

The demonstration of permanent periodic refractive index perturbations along the core of an optical fiber, and their application as narrowband reflection filters, was first reported by Hill *et al.* in 1978 [1]. This effect has subsequently been the basis of extensive research and commercial efforts and allowed the development of an extensive range of optical devices used, for example, in various telecommunications and sensing applications [2–4]. These devices, commonly known as fiber Bragg gratings (FBGs), exhibit a wide variety of characteristics as determined by a number of parameters, including the fabrication methodology and the geometrical and material properties of the optical fiber.

FBGs are typically inscribed via the side illumination of a short length of the core of an optical fiber using suitable laser light. This results in small changes in the core refractive index, the extent of which is related to the integrated fluence at a given point. Because of the many possible variations in the process FBGs may be described in several ways, including the manner in which the refractive index of the core of the fiber changes with time, e.g., type I, type II, and as influenced by the beam intensity [5]; whether the irradiation is via an ultraviolet cw (or quasi-cw) beam or high-intensity femtosecond-scale pulses; or in terms of variations in the resultant spectral properties compared with standard FBGs, i.e., chirped FBGs, π -phase-shifted FBGs, and superstructure FBGs [3].

The behavior of all such Bragg gratings arises from the interaction of a forward propagating fiber mode with the periodic refractive index variation along the fiber core. At, or near, one of the FBG resonances there is a strong coupling into the corresponding reflected backward mode, at a wavelength that is given by [2]

$$\lambda(m) = \frac{2}{m} n_{\text{eff}} \Lambda, \quad (1)$$

where Λ is the grating period along the fiber core and the harmonic number $m = 1, 2, 3, \dots$. The effective index of the

fundamental fiber mode, n_{eff} , can be approximated as the refractive index of the fiber core at $\lambda(m)$. The so-called Bragg wavelength, λ_B , is the wavelength of the first-harmonic resonance (i.e., $m = 1$).

The side-exposure method of FBG writing usually involves illumination of a short fiber length with an interferogram to generate the required refractive index periodicity. Alternatively, the point-by-point writing approach employing precision mechanical translation stages and controls can be adopted. A common method to obtain the interferogram is via insertion of a phase mask (PM) in the beam, which is popular because it is straightforward, repeatable, requires relatively few precision components, and produces a well-defined periodicity of $\Lambda = \Lambda_{\text{pm}}/2$ along the fiber core [3]. Standard phase masks are designed to provide maximum contrast for the interference of the ± 1 diffraction orders, through elimination of the zero and higher orders. However, in most phase masks these undesired orders are not totally suppressed. As a result, phase-mask-produced FBGs have a complex refractive index structure, as observed in images obtained of gratings [6,7]. There are co-existing FBG periods of $\Lambda = \Lambda_{\text{pm}}/2$ and Λ_{pm} present in the interference field behind a phase mask, as noted in simulations [8]. Furthermore, through the Talbot effect, diffraction patterns exhibit a repeat distance known as the Talbot length, L_T [8]; for standard phase masks this length arises from the interaction of the ± 1 and ± 2 orders [9]. Indeed, images of FBGs obtained via the differential interference contrast method, which exhibited these co-existing FBG periodicities ($\Lambda_{\text{pm}}/2$ and Λ_{pm}), have been replicated by modeling based on the strengths of the phase mask's diffraction orders [9]. Across a Talbot period the dominant periodicity along the FBG is Λ_{pm} , which manifests as two interleaved (i.e., π out-of-phase) gratings that produces the $\Lambda_{\text{pm}}/2$ periodicity in the region where they overlap [9,10]. Spectrally, the grating resonances will be the harmonics of the Bragg wavelength and double the Bragg wavelength:

$$\lambda(m) = \frac{n_{\text{eff}}}{m} \Lambda_{\text{pm}} = \frac{\lambda_B}{m}, \quad (2a)$$

$$\lambda(m) = \frac{2n_{\text{eff}}}{m} \Lambda_{\text{pm}} = \frac{2\lambda_B}{m}. \quad (2b)$$

Indeed FBGs resonances in phase-mask-produced gratings have been observed at double the Bragg wavelength [11,12] and at several of the harmonics of either the Bragg wavelength or twice the Bragg wavelength, namely $2\lambda_B/3$, $\lambda_B/2$ and $2\lambda_B/5$ [10,13]. On the other hand, when just the ± 1 diffraction orders were present in an FBG writing arrangement involving a Talbot interferometer, features at twice the Bragg wavelength (expected near 1550 nm for $\Lambda_{\text{pm}} = 536$ nm) were not observed [14].

In order to study reflection peaks or transmission dips at wavelengths other than the Bragg wavelength it is useful to ensure the fiber is single-moded at such wavelengths. This removes the potential complication of higher-order mode effects on the spectral details and thus, for a standard FBG, a single narrowband peak is expected. However, in previous work by the authors and others there are a number of examples where different harmonics of the Bragg wavelength have two closely spaced peaks despite the fiber being single-moded, while a single peak is observed at the Bragg wavelength [11,15,16]. It has been proposed that this double-peak structure arises from the interleaved π out-of-phase grating planes of periodicity Λ_{pm} (as discussed above), which produces a type of π -phase-shifted FBG in which the normal reflection peak has a dip at its center due to reflections from neighboring planes being cancelled [12]. It is important to note that these interference effects between out-of-phase grating planes occur only for the odd harmonics of Eq. (2b), (i.e., $2\lambda_B$, $2\lambda_B/3$, $2\lambda_B/5$) and so double peaks are never present for the harmonics of Eq. (2a) (i.e., λ_B , $\lambda_B/2$, $\lambda_B/3$).

Interestingly, Dyer *et al.* [11] in summarizing their experiments (in which they reported on damage gratings using 193 nm radiation in fiber of unspecified diameter), noted the occurrence of either a single peak or a double peak at $2\lambda_B$ in different gratings. They attributed the double peak to fiber misalignment, noting that a 1 mrad angle between the phase mask surface and the fiber produced a separation between the two peaks of ~ 1 nm, meaning that the Talbot planes were not co-linear with the fiber axis. They conjectured that this produced a Fabry–Perot cavity in which a transmission maximum occurred at the grating reflectance peak since certain grating planes of periodicity Λ_{pm} were π out-of-phase with similar planes elsewhere along the fiber core [11]; such a condition will not occur for perfect alignment. This and the previous descriptions are virtually equivalent, as standard π -phase-shifted gratings are a Fabry–Perot effect arising from two distinct grating sections along the fiber core that are shifted in phase with respect to each other, and which usually, through a large value of the DC refractive index change, have a very narrow passband in the middle of the grating's transmission dip [17]. As the grating operating at twice the Bragg wavelength arises through the presence of phase mask diffractive orders other than ± 1 , the refractive index change is small resulting in a passband peak in the middle of their transmission spectrum that is relatively broad. Modeling of this provided a good account of why the transmission

spectrum at twice the Bragg wavelength is essentially a pair of dips [18]. Unfortunately, although Dyer *et al.* showed that the Talbot length was $\sim 5 \mu\text{m}$ they did not provide details of the fiber diameter or of the conjectured Fabry–Perot cavity. Nevertheless, their work suggests that spectral details, at twice the Bragg wavelength and at wavelengths given by Eq. (2b), are affected if there is a nonzero angle between the Talbot planes and the fiber axis. Knowing the actual fiber diameter is also important as, clearly, it determines how many Talbot planes are present in the fiber core [19]. This may also influence spectra as shown for investigations of fibers with different core diameters, for which the spectra had very different characteristics [12,20]. The propagation of a guided mode through the complex refractive index pattern has yet to be studied in detail, although for multimoded planar devices it has been shown that interleaved grating planes can operate as mode-selective reflectors [21].

The presence of two peaks at double the Bragg wavelength was, as noted above, attributed to the alignment of the FBG writing system [11], and this might be why the peak/dip spacing at twice the Bragg wavelength changed from 0.3 nm in a stationary writing system [12] to 0.45 nm when a scanning method was used, despite all gratings being written with the same phase mask and fiber type [22]. Indeed the alignment of optical components in FBG fabrication systems has been shown by other authors to be responsible for small changes in spectra near the Bragg wavelength. For example, it was shown that small deviations ($\pm 0.01^\circ$) of the UV laser beam from normal incidence on the phase mask had a significant effect on free-space interference patterns [8], while the effect of an angular misalignment with respect to the phase mask of the input beam was simulated for three-dimensional interference patterns [23]. Furthermore, it was found that the Bragg wavelength was shorter in the case of a converging incident beam and longer when the incident light was diverging [24]. The deliberate tilting of the phase mask with respect to the fiber, at an angle of about 4° or greater, results in the formation of a blazed grating in which some of the reflected power is reflected into cladding modes [25] and the Bragg wavelength increases slightly [Eq. (1) is multiplied by $1/\cos \theta$, where θ is the tilt angle] [26]. This paper presents results of investigations of how the double-peak properties at harmonics of the Bragg wavelength are related to the writing conditions. To do this, investigations of the alignment and positioning of the fiber with respect to the phase mask were conducted, to observe how the FBG spectra, and in particular the wavelength spacing of dual peaks, were affected. In each case the fiber core was exposed to a particular portion of the three-dimensional complex diffraction pattern produced by a standard phase mask.

2. EXPERIMENTAL DETAILS

A series of FBGs were fabricated using a 244 nm UV continuous laser source with the scanning beam direct writing method. Two different phase masks were investigated, the first of which had a 536 nm pitch (PM1). The measured average relative strengths of the PM1 0th, ± 1 , and ± 2 diffraction orders were 3.0%, 31.2%, and 17.3%, respectively, and the Talbot length was calculated to be $\sim 1.0 \mu\text{m}$ (for the interference of the ± 1 and ± 2 orders). The second phase mask studied had a pitch of $1.0703 \mu\text{m}$ (PM2). For this phase mask

the measured average relative strengths of the PM2 0th, ± 1 , and ± 2 diffraction orders were 4.1%, 44.3%, and 3.7%, respectively, and the Talbot length was calculated to be $\sim 4.6 \mu\text{m}$ for the combination of ± 1 and ± 2 orders. Two different fiber types were investigated allowing effects to be studied at a range of wavelengths while ensuring single-mode operation. As in previous work, Corning HI 1060 FLEX fiber, with a core diameter of $3.4 \mu\text{m}$, a mode field diameter $4 \mu\text{m}$ at 980 nm, and a cutoff wavelength of 930 nm was used. In addition, gratings were written in Nufern GF1 fiber with a mode field diameter of $10.5 \mu\text{m}$ (at 1550 nm) and a cutoff wavelength of 1260 nm. All of the fibers tested were preloaded with hydrogen to increase the photosensitivity. The length of each FBG was chosen to be 5 mm.

Reflection spectra were measured at a range of different wavelengths corresponding to various harmonics of the Bragg wavelength. To cover the range of wavelengths of interest, several different experimental configurations were required. Peaks in the 1550 nm region were monitored using a swept wavelength system (JDS Uniphase, SWS15100) having a resolution of 3 pm. For the other wavelength ranges of interest, spectra were measured using an appropriate light source and an optical spectrum analyzer (ANDO, AQ6317B) in reflection mode using a 2×2 coupler. For peaks near 785 nm a superluminescent diode (780 nm center wavelength, FWHM 45 nm) was used while the remaining wavelengths were covered by the output from a supercontinuum white light source (Fianium Femtopower 1060). Although absolute reflectance values are provided in spectra, caution must be followed when attempting a direct comparison of peak reflectance values obtained for different gratings since the magnitude of the reflectance peaks for the standard writing of Bragg gratings depends upon conditions including writing time, writing power, and hydrogen loading. Indeed the peak reflectance at harmonics of the Bragg wavelength depends upon the fiber type used [10,19].

Software routines were developed specifically to analyze the measured spectra. The center wavelengths of reflectance peaks, above a set threshold level, were calculated as the mid-wavelength point of the 50% peak reflectance levels. The wavelength separation between dual peaks was simply determined from the difference in the center wavelengths of the peaks. The FWHM of peaks was calculated as the distance between the 50% peak level points.

Examples of FBG spectra at different harmonics of the Bragg wavelength are shown in Figs. 1 and 2, for gratings

written with PM1 and PM2, respectively. The Bragg wavelength for the PM1 is approximately 780 nm and, as expected, a single but somewhat saturated peak is observed [Fig. 1(a)] for a grating written in GF1 fiber. At twice the Bragg wavelength, two peaks are observed [Fig. 1(b)]. For gratings written with PM2, the Bragg wavelength is approximately 1550 nm, and a single peak is seen for gratings written in both HI 1060 FLEX and GF1 fiber at this wavelength [Figs. 2(c) and 2(f), respectively]. As expected, two peaks are observed for the $2\lambda_B/3$ harmonic of PM2 near 1040 nm [Figs. 2(b) and 2(e)], while single peaks were obtained in both fiber types at half the Bragg wavelength at ~ 780 nm [Figs. 2(a) and 2(d)]. The narrower peaks obtained at the harmonics of the Bragg wavelength (i.e., $2\lambda_B$, $2\lambda_B/3$, $\lambda_B/2$) are indicative of lower reflectances compared to those obtained at the Bragg wavelength for a particular optical fiber and phase mask configuration.

The arrangements used to study grating writing conditions are illustrated in Fig. 3. Initially the phase mask was vertical, the fiber was horizontal and parallel to the phase mask, and the UV beam direction was perpendicular to both. The precision of the initial alignments of all of these relative orientations was limited by manual alignment processes. In the first investigation, A, FBGs were written with the fiber at various distances, d , from the phase mask with the fiber remaining horizontal and parallel to the phase mask [as shown in Figs. 3(a) and 3(d)]. A range of changes in the fiber to phase mask distance were tested, including looking at the effect of small steps (of the order of $1 \mu\text{m}$) and gross changes (up to $100 \mu\text{m}$) from the original fiber alignment (fiber to phase mask distance $\sim 100 \mu\text{m}$). For investigation B, FBGs were written as the phase mask was rotated at an angle, θ , about the UV beam direction by up to approximately $\pm 4^\circ$, while keeping the fiber horizontal, and at a uniform distance of $\sim 100 \mu\text{m}$ from the phase mask [as shown in Figs. 3(b) and 3(e)]. Positive and negative angles refer to clockwise and anticlockwise rotations, respectively, relative to vertical. In this investigation a photo was taken of the phase mask relative to the horizontal fiber for each grating written, which was subsequently used to determine the exact angles of the phase mask. Finally, in investigation C, the fiber alignment was adjusted so that one end of the fiber was closer to the phase mask than the other end, while keeping the fiber horizontal and the phase mask unrotated, i.e., $\theta = 0^\circ$ [as shown in Figs. 3(c) and 3(f)]. Gratings were written for fiber to phase mask angles, ϕ , of up to $\pm 0.11^\circ$, where the positive angle refers to the

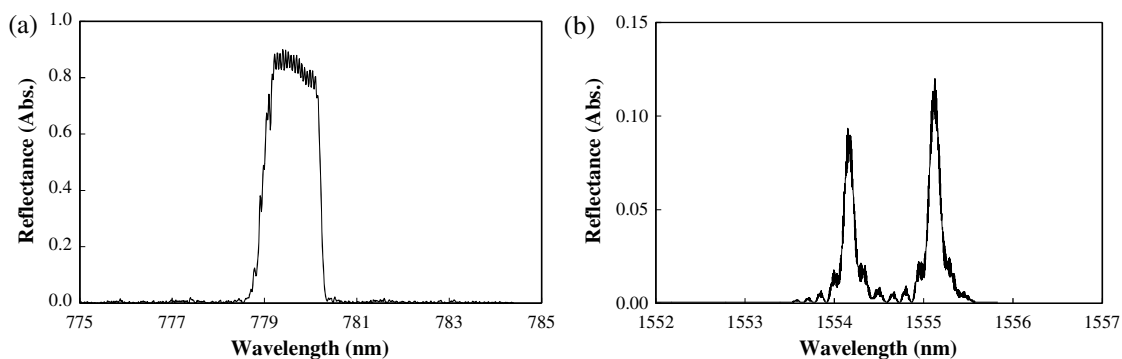


Fig. 1. Examples of spectra at (a) the Bragg wavelength and (b) twice the Bragg wavelength for gratings written in HI 1060 FLEX fiber with the 536 nm pitch phase mask (PM1).

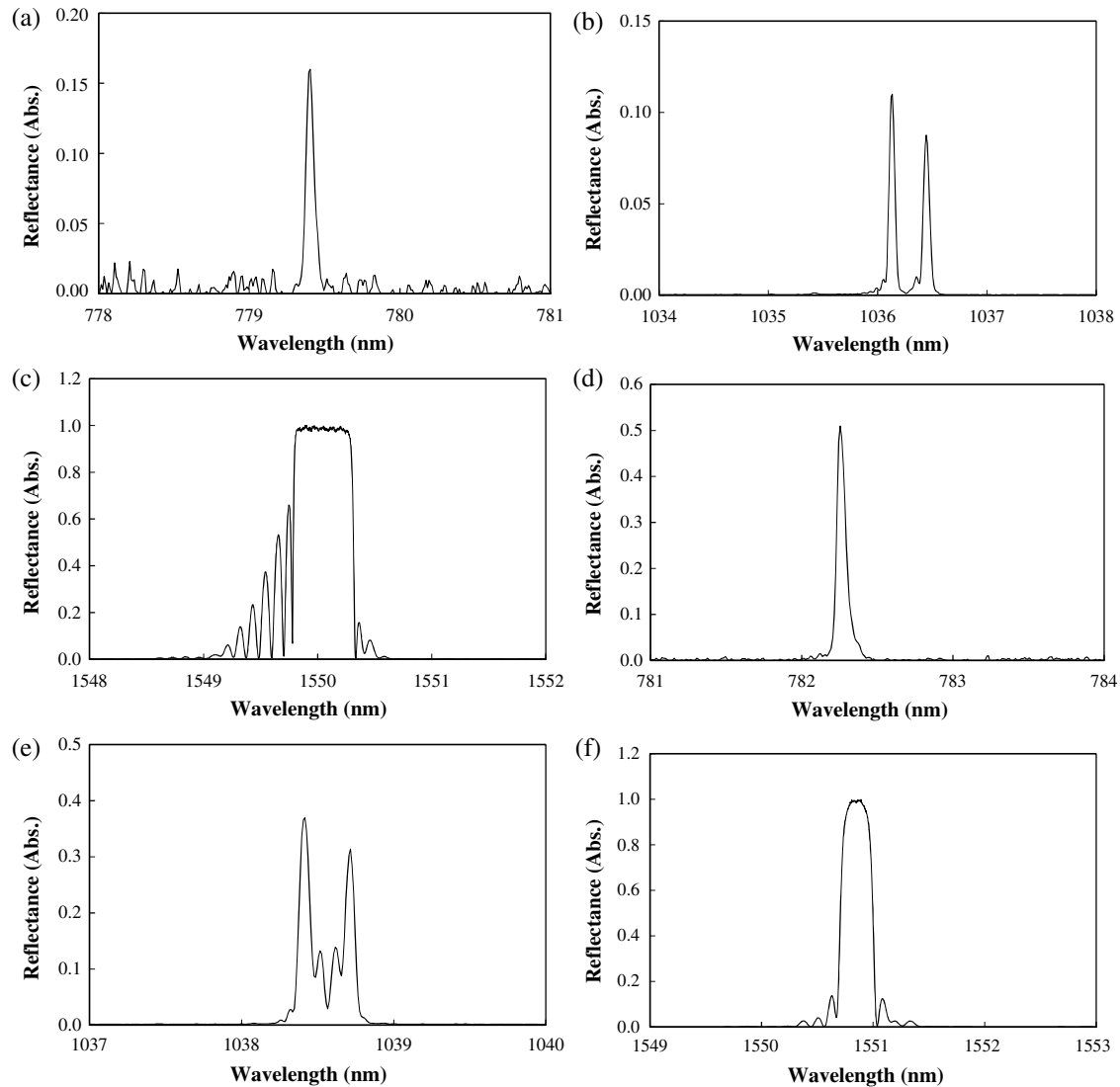


Fig. 2. Examples of spectra at (a) half the Bragg wavelength and (b) $2/3$ the Bragg wavelength and (c) the Bragg wavelength for gratings written in GF1 fiber, (d) at half the Bragg wavelength and (e) $2/3$ the Bragg wavelength and (f) the Bragg wavelength for gratings written in HI 1060 FLEX fiber with the $1.0703 \mu\text{m}$ pitch phase mask (PM2).

right-hand side of the fiber moving away from the phase mask, while negative angles refer to the left-hand side of the fiber moving away from the phase mask. The automated positioning stages used in the fiber alignment (Newport MFN25CC) allowed control with a resolution of approximately $1 \mu\text{m}$. For the fiber angle tests this step size equates to an angle resolution of approximately $2 \times 10^{-4}^\circ$.

3. RESULTS

A. Variation of Distance Between Fiber and Phase Mask

As shown in Figs. 3(a) and 3(d), the aim of this experiment was to determine whether FBG spectra were affected by having the fiber core exposed to slightly different regions of the diffraction field during writing, which might involve contributions from different numbers of Talbot planes, and change which phase mask orders were contributing [9,19]. Gratings were written in both the GF1 and HI 1060 FLEX fiber with PM2, and in HI 1060 FLEX fiber with PM1. For the FBGs written with PM2, the dual peaks were observed

and measured at the $2\lambda_B/3$ harmonic of the Bragg wavelength at approximately 1040 nm. For the FBGs written with PM1, the dual peaks were observed at the $2\lambda_B$ harmonic of the Bragg wavelength at approximately 1555 nm. No clear changes in either the center wavelengths or the spacing between the dual peaks were observed over the ranges tested for any of the fiber/phase mask combinations studied. The maximum variations in peak spacing were of the order of 0.1 nm but were uncorrelated with respect to fiber offset distance.

B. Rotation of Phase Mask

The effect of phase mask rotation on FBG spectra was investigated for gratings written in HI 1060 FLEX fiber using PM1 using the $2\lambda_B$ harmonic of the Bragg wavelength at approximately 1555 nm. Examples of spectra obtained for gratings written with phase mask rotation angles in the range between -4° and $+4^\circ$ are shown in Fig. 4. The rotation of the phase mask is expected to produce blazed gratings, as illustrated in Fig. 3(e). In Fig. 5(a) the change in center wavelength for each of the two peaks with respect to the orientation angle

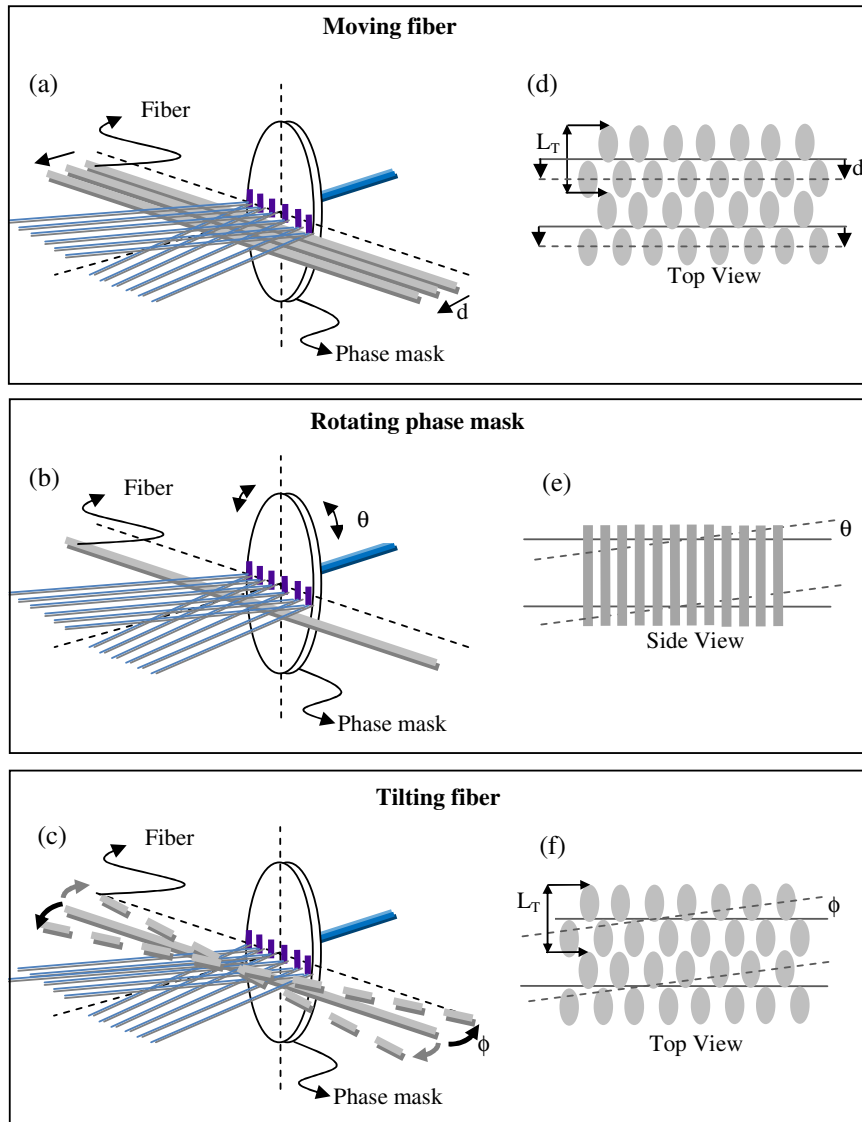


Fig. 3. (Color online) Schematic of the three experimental investigations [(a), (b), and (c)] and for each of these the manner in which the fiber core is being moved within the phase mask diffraction field [(d), (e), and (f)], respectively: (a) and (d) moving the fiber away from the phase mask, (b) and (e) tilting of the phase mask about the laser beam, and (c) and (f) inclining the fiber at an angle with respect to the phase mask.

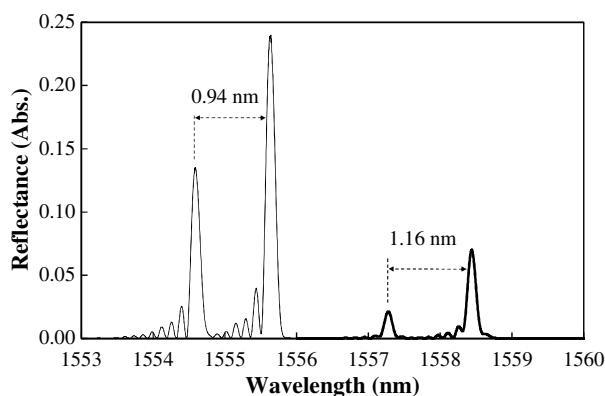


Fig. 4. Examples of spectra for rotating the phase mask for gratings written in HI 1060 FLEX fiber with the 536 nm pitch phase mask (PM1) at minimum rotation angle ($\sim 0^\circ$, thin line) and maximum rotation angle ($\sim 3.9^\circ$, thick line).

of the phase mask is shown. The two reflection peaks show a clear shift in center wavelength with an obvious spacing between the two peaks. The dashed lines in Fig. 5(a) are the calculated wavelengths when the peak wavelengths near 0° were divided by the cosine of the phase mask orientation angle, corrected for the slight offset, as appropriate for blazed gratings [26]. This has the correct trend but slightly overestimates the observed wavelength variation.

The magnitude of wavelength spacing between the two peaks is plotted in Fig. 5(b) as a function of the phase mask rotation angle. The results show a clear relationship between the phase mask orientation angles and the spacing between the two main peaks. The dashed line in Fig. 5(b) is a linear fit to the data, which gives a gradient of -0.06 nm/deg. The average FWHM measured for each of the individual reflectance peaks was approximately 0.14 nm. No obvious trends in FWHM with phase mask angle were observed.

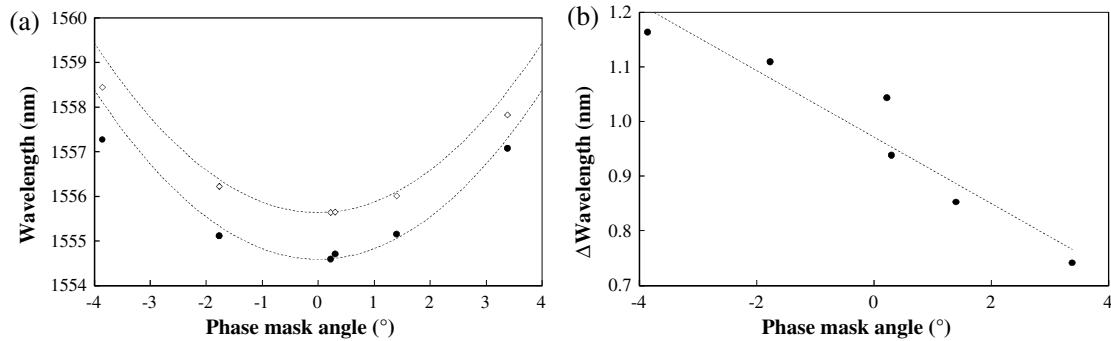


Fig. 5. Results at twice the Bragg wavelength for when the phase mask was rotated for (a) the wavelength of the two peaks and (b) their separation, for gratings written with HI 1060 FLEX fiber and PM1 combination. The dashed line in (a) is a fit of $1/\cos \theta$, and in (b) a linear trend line.

C. Tilting of Fiber with Respect to the Phase Mask

Tests investigating tilting the optical fiber were performed with two combinations of phase mask and optical fiber type. In one combination, gratings were written in GF1 fiber using PM2, and the spectra for the $2\lambda_B/3$ harmonic of the Bragg wavelength at approximately 1040 nm were examined. The other combination involved writing gratings in HI 1060 FLEX fiber with PM1 and studying the $2\lambda_B$ harmonic of the Bragg wavelength at approximately 1555 nm. When analyzing the spectra a clear dependence of the wavelength separation of the dual peaks on the fiber angle relative to the phase mask was observed, with a single peak present when the angle was close to zero. Examples of spectra obtained for dual and single peaks for both fiber/phase mask combinations tested are shown in Fig. 6. The average FWHM measured for each of the individual reflectance peaks was approximately 0.06 nm for FBG written in GF1 fiber using PM2 and 0.13 nm

for FBG written in HI 1060 FLEX fiber with PM1. No obvious trends in FWHM with fiber to phase mask angle were observed.

The shift in the center wavelength for each of the two peaks with respect to the fiber tilt angle is shown in Figs. 7(a) and 8(a) for the two different fiber/phase mask combinations tested, while Figs. 7(b) and 8(b) show the wavelength separation differences of the two peaks at each angle. Given the uncertainty in determining this alignment with high precision, the symmetry of these data allowed 0° to be assigned to the case when there was a single peak. While the average of the peak wavelengths is virtually unchanged with tilt angle, their separation exhibits a rapid and linear variation with tilt angle with a negative gradient for negative fiber angles and a positive gradient for positive fiber angles. The magnitudes of the gradients of wavelength difference with fiber angle were virtually identical for positive and negative fiber angles. Linear

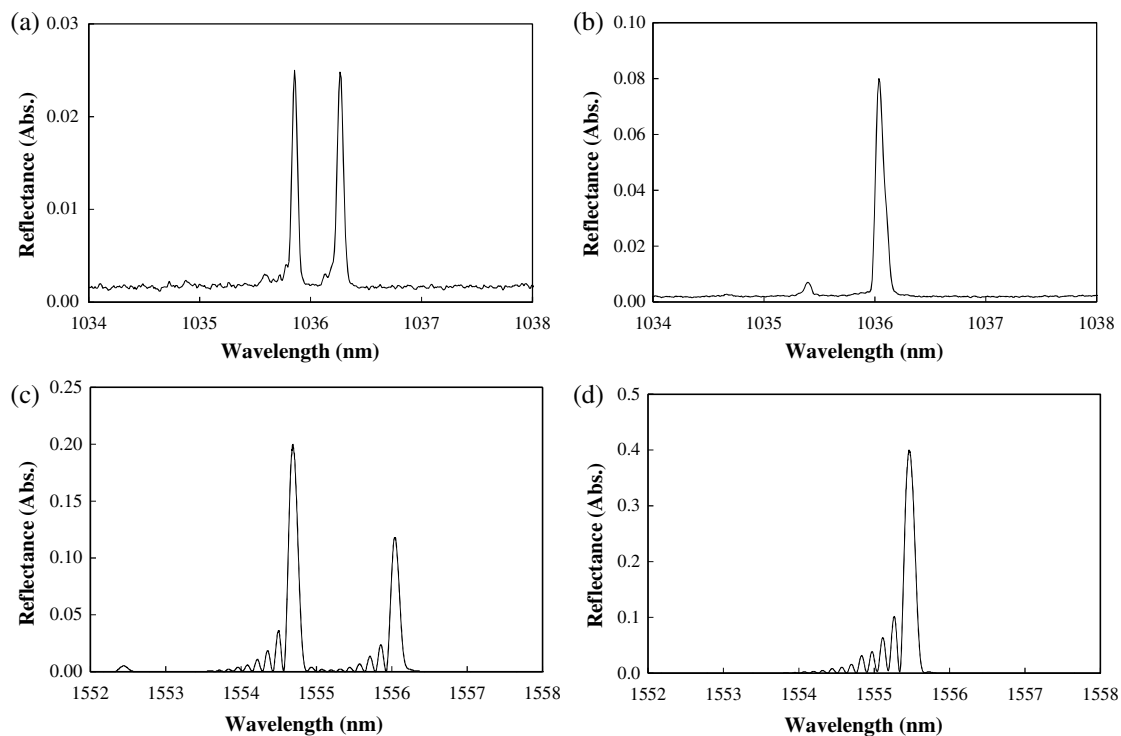


Fig. 6. Examples of spectra for tilting the fiber relative to the phase mask for GF1 fiber and $1.0703 \mu\text{m}$ phase mask at (a) peak separation (fiber angle $\sim 0.07^\circ$) and (b) single peak (fiber angle $\sim 0^\circ$) and for HI 1060 FLEX fiber and 536 nm phase mask at (c) peak separation (fiber angle $\sim -0.10^\circ$) and (d) single peak (fiber angle $\sim 0^\circ$).

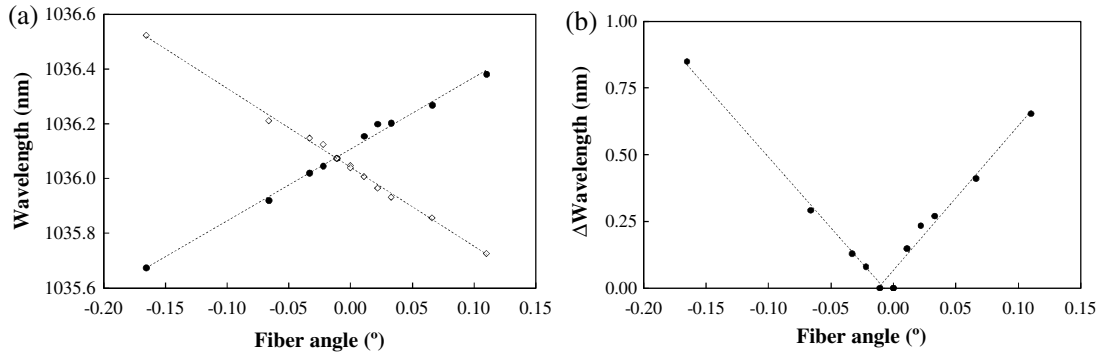


Fig. 7. Results for the GF1 fiber and 1.0703 μm phase mask for when the fiber was tilted for (a) the individual wavelengths of the two peaks and (b) their wavelength separation. The dashed lines are linear fits to the data.

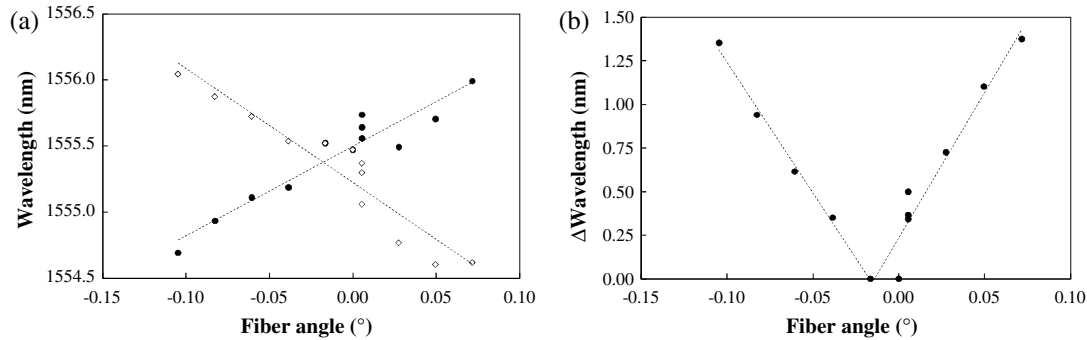


Fig. 8. Results for the HI 1060 FLEX fiber and 536 nm phase mask for when the fiber was tilted for (a) the individual wavelengths of the two peaks and (b) their wavelength separation. The dashed lines are linear fits to the data.

fits to the peak wavelength separations gave average normalized gradients of 5.4 nm/deg for the GF1 fiber/PM2 data and 15.8 nm/deg for the HI 1060 FLEX fiber/PM1 data.

Figure 3(f) depicts the situation of having the Talbot planes parallel with the fiber core, illustrating the condition described by Dyer *et al.* as being aligned [11]. Conversely, if alignment is not achieved the fiber core will pass through successive Talbot planes at a rate that depends upon the angle. Our data (Figs. 7 and 8) exhibits a sensitivity of the wavelength variation with angle that is much greater than that evident in Fig. 5(b) for the phase mask angle tests, with double peaks occurring when the angle is $\geq 0.01^\circ$. Clearly the occurrence of a single peak [i.e., Figs. 6(b) and 6(d)] is a special condition, supporting the assertion of Dyer *et al.* very strongly. Images of the complex refractive index patterns in such FBGs would be useful to provide further verification.

4. DISCUSSION

Thus it is clear that slight variations in FBG writing conditions affect the behavior of the two peaks at double the Bragg wavelength (or at the odd harmonics of this) significantly. These results are consistent with earlier work, where a rotation in the cylindrical lens changed the separation between the peaks and there was a split from a single peak to two peaks [27], and with the finding that slight variations in the incoming UV light directions causes changes in FBG spectral details [8].

More significantly, the results provide strong support for the suggestion of Dyer *et al.* that the double peaks observed at twice the Bragg wavelength, or at odd harmonics of this,

arise because the alignment of the fiber core is not exactly perpendicular to the Talbot diffraction pattern generated by the phase mask [11]. Spectral properties at these wavelengths depend upon how the Talbot diffraction pattern generated by the phase mask, consisting of perfectly interleaved grating planes all of periodicity Λ_{pm} (i.e., adjoining planes are π out-of-phase), is photo-imprinted on the photosensitive fiber core. Perfect alignment enables a given Talbot plane to exist for the full length of the FBG, while any other alignment will cause any Talbot plane to eventually meet the core-cladding boundary. For the combinations of fiber types and phase masks used, the Talbot length, L_T , was less than or comparable with the core diameter, which means that across the fiber diameter at any given position both phases of the grating planes (of periodicity Λ_{pm}) exist [19] and which, when the alignment is not perfect, produces two peaks at twice the Bragg wavelength, as noted previously [11,12]. Although consideration of destructive interference between waves reflected from out-of-phase gratings gives a qualitative account for the two peaks arising due to a dip in the usual grating reflection peak, it does not account for why the separation of the two peaks depends upon the tilt angle, ϕ . A full account of why there are two peaks that diverge as ϕ increases is needed, but is beyond the scope of this work. It may be that the propagating mode encounters two different grating periodicities, which depend upon $\sin \phi$ (i.e., approximated by ϕ for the very small angular range investigated) and when only a single peak occurs at $2\lambda_B$ there is just one periodicity and the system may be regarded as aligned. Although Dyer *et al.* proposed a Fabry–Perot effect [11], they provided limited details.

We note that for their work, the reported peak separation of 1 nm implies a cavity length of ~ 0.8 mm. When an FBG is not aligned properly the guided mode (at twice the Bragg wavelength or its odd harmonics) in the core encounters a succession of adjoining out-of-phase grating planes (of periodicity Λ_{pm}) that, by consideration of the geometry of Fig. 3(f), exhibits a periodicity of $L_T / \sin \phi$ along the fiber core. For the work of Dyer *et al.* we calculate this distance to be ~ 5 mm, which is very different to the inferred Fabry–Perot cavity length of 0.8 mm. Thus, whether a Fabry–Perot effect is the cause requires further investigation that will necessarily involve consideration of related studies, such as the behavior of pairs of FBGs used as in-fiber Fabry–Perot cavities [28], and consideration of the coherence length of the light source [29].

These studies have shown that the differences in dual peak wavelength separation values for FBGs written with the same phase mask and optical fiber combination obtained in previous work [12,20,22] are due to differences in fiber alignment. The data obtained also suggest that controlled changes in writing conditions can be used to produce FBGs with specific properties, which may be useful for sensing and other applications.

Last, it might be inferred that these results provide for a method for ensuring the alignment of an FBG writing system. However, even if true alignment has been obtained, by virtue of a single peak at twice the Bragg wavelength, this does not guarantee that the replacement of a fiber with a new fiber will result in proper alignment as slight variations are inevitable when a new optical fiber is mounted in the system.

5. CONCLUSIONS

Sets of FBGs have been fabricated in two different fiber types and using two phase masks of very different pitch. This allowed the effects of three different alignment variations of the optical fiber with respect to the phase mask on the double-peak structure that had been reported at twice the Bragg wavelength (and at odd harmonics of this) to be investigated. Most significantly, the situation of there being only one peak at twice the Bragg wavelength, which Dyer *et al.* described as being aligned [11], was verified by measurements of wavelength separation as the angle between the fiber and the phase mask surface was changed. Indeed, the alignment sensitivity is such that if the Talbot planes are not perfectly parallel with the fiber axis then two peaks are present, as found when the angle between the fiber and the phase mask surface was less than 0.1 mrad. In contrast to this extreme sensitivity with alignment angle, the rotation of the phase mask provided a much less sensitive $1/\cos \theta$ variation of the wavelength with angle, due to blazed gratings being produced in which the grating planes are not perpendicular to the fiber axis, as expected. The results demonstrate that FBG spectra at twice the Bragg wavelength are highly sensitive to the actual relationship between the Talbot diffraction pattern and the fiber core. Further work in understanding these gratings is in progress, particularly for accounting for the variation of the peak separation at double the Bragg wavelength (or at the odd harmonics of this) with the angle, ϕ , between the fiber and the phase mask, as well as examination of their properties in different fiber types [30]. Investigations of the response of such gratings to various measurands has also been reported for comparison with standard FBGs [31].

ACKNOWLEDGMENTS

The authors would like to acknowledge the financial support of the Australian Research Council.

REFERENCES

1. K. O. Hill, Y. Fuji, D. C. Johnson, and B. S. Kawasaki, "Photosensitivity in optical fiber waveguides: Application to reflection filter fabrication," *Appl. Phys. Lett.* **32**, 647–649 (1978).
2. K. O. Hill and G. Meltz, "Fiber Bragg grating technology fundamentals and overview," *J. Lightwave Technol.* **15**, 1263–1276 (1997).
3. A. Othonos and K. Kalli, *Fiber Bragg Gratings* (Artech House, 1999).
4. A. D. Kersey, M. A. Davis, H. J. Patrick, M. LeBlanc, K. P. Koo, C. G. Askins, M. A. Putnam, and E. J. Friebele, "Fiber grating sensors," *J. Lightwave Technol.* **15**, 1442–1463 (1997).
5. J. Canning, "Fibre gratings and devices for sensors and lasers," *Laser Photon. Rev.* **2**, 275–289 (2008).
6. N. M. Dragomir, C. Rollinson, S. A. Wade, A. J. Stevenson, S. F. Collins, G. W. Baxter, P. M. Farrell, and A. Roberts, "Nondestructive imaging of a type I optical fiber Bragg grating," *Opt. Lett.* **28**, 789–791 (2003).
7. C. W. Smelser, S. J. Mihailov, D. Grobncic, P. Lu, R. B. Walker, H. Ding, and X. Dai, "Multiple-beam interference patterns in optical fiber generated with ultrafast pulses and a phase mask," *Opt. Lett.* **29**, 1458–1460 (2004).
8. J. D. Mills, C. W. J. Hillman, B. H. Blott, and W. S. Brocklesby, "Imaging of free-space interference patterns used to manufacture fiber Bragg gratings," *Appl. Opt.* **39**, 6128–6135 (2000).
9. B. P. Kouskousis, C. M. Rollinson, D. J. Kitcher, S. F. Collins, G. W. Baxter, S. A. Wade, N. M. Dragomir, and A. Roberts, "Quantitative investigation of the refractive-index modulation within the core of a fiber Bragg grating," *Opt. Express* **14**, 10332–10338 (2006).
10. C. M. Rollinson, S. A. Wade, N. M. Dragomir, G. W. Baxter, S. F. Collins, and A. Roberts, "Reflections near 1030 nm from 1540 nm fibre Bragg gratings: Evidence of a complex refractive index structure," *Opt. Commun.* **256**, 310–318 (2005).
11. P. E. Dyer, R. J. Farley, R. Giedl, K. C. Byron, and D. Reid, "High reflectivity fibre gratings produced by incubated damage using a 193 nm ArF laser," *Electron. Lett.* **30**, 860–862 (1994).
12. S. P. Yam, Z. Brodzeli, B. P. Kouskousis, C. M. Rollinson, S. A. Wade, G. W. Baxter, and S. F. Collins, "Fabrication of a π -phase-shifted fiber Bragg grating at twice the Bragg wavelength with the standard phase mask technique," *Opt. Lett.* **34**, 2021–2023 (2009).
13. B. Malo, D. C. Johnson, F. Bilodeau, J. Albert, and K. O. Hill, "Single-excimer-pulse writing of fiber gratings by use of a zero-order nulled phase mask: grating spectral response and visualization of index perturbations," *Opt. Lett.* **18**, 1277–1279 (1993).
14. S. P. Yam, Z. Brodzeli, S. A. Wade, G. W. Baxter, and S. F. Collins, "Occurrence of features of fiber Bragg grating spectra having a wavelength corresponding to the phase mask periodicity," *J. Electron. Sci. Technol.* **6**, 458–461 (2008).
15. C. M. Rollinson, S. A. Wade, N. M. Dragomir, A. Roberts, G. W. Baxter, and S. F. Collins, "Three parameter sensing with a single Bragg grating in non-birefringent fiber," in *Proceedings of Topical Meeting on Bragg Gratings, Poling, and Photosensitivity (BGPP)* (Engineers Australia, 2005), pp. 92–94.
16. S. P. Yam, C. M. Rollinson, D. J. Kitcher, G. W. Baxter, and S. F. Collins, "Transverse strain response of transmission dips at 2/3 of the Bragg wavelength in a fiber Bragg grating," in *18th International Conference on Optical Fiber Sensors* (Optical Society of America, 2006), paper TuE47.
17. J. Canning and M. G. Sceats, "Pi-phase-shifted periodic distributed structures in optical fibres by UV post-processing," *Electron. Lett.* **30**, 1344–1345 (1994).
18. S. P. Yam, G. W. Baxter, S. A. Wade, and S. F. Collins, "Modelling of an alternative pi-phase-shifted fibre Bragg grating operating at twice the Bragg wavelength," in *35th Australian Conference on Optical Fibre Technology (ACOFT), 2010* (Australian Institute of Physics, 2010), p. 659.

19. C. M. Rollinson, S. A. Wade, B. P. Kouskousis, D. J. Kitcher, G. W. Baxter, and S. F. Collins, "Variations of the growth of harmonic reflections in fiber Bragg gratings fabricated using phase masks," *J. Opt. Soc. Am. A* **29**, 1259–1268 (2012).
20. H. K. Bal, N. M. Dragomir, F. Sidirolou, S. A. Wade, G. W. Baxter, and S. F. Collins, "Response of some pi-phase-shifted Bragg gratings to elevated pressure," *Proc. SPIE* **7753**, 775389 (2011).
21. S. Tomljenovic-Hanic and J. D. Love, "Symmetry-selective reflection gratings," *J. Opt. Soc. Am. A* **22**, 1615–1619 (2005).
22. H. K. Bal, F. Sidirolou, Z. Brodzeli, S. A. Wade, G. W. Baxter, and S. F. Collins, "Fibre Bragg grating transverse strain sensing using reflections at twice the Bragg wavelength," *Meas. Sci. Technol.* **21**, 094004 (2010).
23. P. E. Dyer, R. J. Farley, and R. Giedl, "Analysis and application of a 0/1 order Talbot interferometer for 193 nm laser grating formation," *Opt. Commun.* **129**, 98–108 (1996).
24. L. Li, L. Zhao, K. Gao, R. Huang, and Z. Fang, "Influence effect of beam divergence on fiber Bragg grating fabricated by UV imprinting," *Acta Opt. Sin.* **22**, 749–752 (2002).
25. R. Kashyap, R. Wyatt, and R. J. Campbell, "Wideband gain flattened erbium fibre amplifier using a photosensitive fibre blazed grating," *Electron. Lett.* **29**, 154–156 (1993).
26. T. Erdogan and J. E. Sipe, "Tilted fiber phase gratings," *J. Opt. Soc. Am. A* **13**, 296–313 (1996).
27. S. P. Yam, Z. Brodzeli, S. A. Wade, G. W. Baxter, and S. F. Collins, "Consistency of optical alignment during FBG fabrication and the spectral responses at twice the Bragg wavelength," in *18th Australian Institute of Physics National Congress (AIP)* (Australian Institute of Physics, 2008), p. 180.
28. S. Legoubin, M. Douay, P. Bernage, P. Niay, S. Boj, and E. Delevaque, "Free spectral range variations of grating-based Fabry-Perot filters photowritten in optical fibers," *J. Opt. Soc. Am. A* **12**, 1687–1694 (1995).
29. S. C. Kaddu, D. J. Booth, D. D. Garchev, and S. F. Collins, "Intrinsic fibre Fabry-Perot sensors based on co-located Bragg gratings," *Opt. Commun.* **142**, 189–192 (1997).
30. H. K. Bal, W. Brown, N. M. Dragomir, S. A. Wade, F. Sidirolou, G. W. Baxter, and S. F. Collins, "Comparison of spectra and images of Bragg gratings written in three different optical fibres," in *Proceedings of the International Quantum Electronics Conference and Conference on Lasers and Electro-Optics IQEC/CLEO Pacific Rim 2011* (Australian Optical Society, 2011), pp. 139–141.
31. S. F. Collins, S. P. Yam, H. K. Bal, B. P. Kouskousis, C. M. Rollinson, F. Sidirolou, Z. Brodzeli, S. A. Wade, and G. W. Baxter, "Fiber Bragg gratings at twice the Bragg wavelength: properties and sensor applications," in *2nd Asia-Pacific Optical Sensors Conference*, Guangzhou, China, 28–30 June 2010.